Fontainebleau/CG N-526

CONDITIONAL SIMULATIONS : A NEW MONTE-CARLO APPROACH TO PROBABILISTIC EVALUATION OF HYDROCARBON IN PLACE

P. DELFINER
J.P. CHILES

Juillet 1977

CONDITIONAL SIMULATIONS : A NEW MONTE CARLO APPROACH TO PROBABILISTIC EVALUATION OF HYDROCARBON IN PLACE

P. DELFINER

J.P. CHILES

Ecole des Mines de Paris - Centre de Géostatistique
35, rue St Honoré - 77305 - FONTAINEBLEAU - FRANCE

ABSTRACT

Conditional simulation is a geostatistical method for generating 2 or 3-dimensional fields of a given variable, that have the same autocorrelation structure as the true field, and are consistent with the observed data. This method is applied to reservoir description parameters, and expectation curves of volumes in place are derived. The field development policy is also examined from the point of view of reserve evaluation.

I - INTRODUCTION

Due to the high cost involved in the acquisition of data on a reservoir, it is of high economical value to get the most out of the information already available. This has motivated the development of more and more sophisticated data processing techniques. Among these, Geostatistics* is a methodology of resources evaluation and planning that has been in use in the Mining Industry for more than fifteen years. Its application to the Petroleum Industry is rather recent however, but it has proved to be a flexible and dependable tool, and is presently being instituted within major companies.

So far, the main application has been the interpolation of reservoir parameters between wells, by the method of "Kriging", in view of contour mapping, volumetric reserve calculations, and input preparation for reservoir simulation models. Geostatistical techniques are also used to process seismic time and velocity data, even in faulted areas, and to update contour maps in a natural and consistent way by means of well-site information, including slopes where a dip-meter logging has been recorded (migration of seismic data). Haas and Jousselin (1975) report several case studies dealing with such applications. Additional references are Haas and Mollier, Haas and Viallix, and except for general theory, this is all, to our knowledge, that has been published on the subject to the attention of petroleum specialists.

We shall not come back here to the applications already mentioned, but rather go further, and apply the newly developed technique of "conditional simulations" to the probabilistic evaluation of hydrocarbon reserves in place. The method is of Monte-Carlo type, with two specific features :

* It seems that the word "Géostatistique" has first been introduced by G. Matheron in 1959 to denote his own approach to estimation problems. Since then, the word has been used in the more general sense of "Statistics in Geology". In this paper, we refer to the original specific meaning.

i) it accounts for the spatial correlations between reservoir parameter data (e.g. permeability, porosity, thickness, saturation)

ii) at well sites, the simulated values are consistent with the measured ones, that is, coincide with them in the absence of measurement errors.

The whole set of numerical values taken by a variable throughout its domain of definition (in two or three dimensions) is simulated at once. Due to the structural information introduced in the model, each of these conditional simulations may be thought of as a "possible" version of the unknown reality, at least as it can be figured out on the basis of the data at hand.

Visualizing several simulations gives an idea of the uncertainty attached to our representation of the spatial distribution of a parameter ; there is an all too strong tendency, once a map is drawn, to accept it as reality. A reservoir geologist may also find it useful to ponder over these several possibilities generated by an objective algorithm, and select one which makes sense to him.

We want here to show how conditional simulations can be used as input to volumetric calculation procedures and lead to the expectation curve of hydrocarbon in place. As secondary consideration , we will also evaluate retrospectively the field development policy from the point of view of the assessment of these reserves. The method will be illustrated on a real, though over-simplified, case study. It should be regarded as a first and necessary attempt before dealing with complex cases.

On the methodological side, the techniques used in the example are quite sophisticated, and this placed the present authors in the uncomfortable situation of having to introduce the more advanced concepts of Geostatistics to readers who may not be familiar with its simpler aspects. The policy has been to avoid duplicating other presentations, and to lay the emphasis on the simulations of a variable with a non-stationary spatial distribution. A presentation of the stationary case can be found in Journel, 1974.

2 - A HURRIED RECOLLECTION

Reservoir parameter data usually show spatial variations that are so complex that only a statistical description can be attempted. A convenient model is to view the set $\{z(x),\ x \in D\}$ of values of a quantity $z(x)$, where x is a point in the domain D, in two or three dimensions, as a realization of a random function $Z(x)$. Furthermore, $Z(x)$ may in turn be modeled as the sum :

$$Z(x) = m(x) + Y(x)$$

of a smooth deterministic function $m(x)$ - the drift or "trend"- and an autocorrelated stationary random fluctuation $Y(x)$, of mean zero.

For some variables, like porosity or thickness, it is reasonable to assume that $m(x) = m$ = constant, for example when D represents a homogeneous layer. Then the inference of the stationary covariance $K(x-y) = E[Z(x)-m][Z(y)-m]$ is relatively easy. As a matter of fact, Geostatistics advocates, rather, the use of the "variogram" :

$$2\,\gamma(x-y) = E[Z(x) - Z(y)]^2$$

because it is a more general and more flexible tool, and has the advantage of not involving the unknown mean m.

The inference problem becomes much more serious when $m(x)$ cannot be considered constant anymore, as in the case, say, for the depth of the top of a dome-shaped structure. The drift is better represented by an expression of the form

$$m(x) = \sum_{\ell=0}^{k} \beta_\ell\, f^\ell(x)$$

where the $f^\ell(x)$ are given functions (usually the monomials of R^2 or R^3) and β_ℓ unknown coefficients. It is tempting to estimate the β_ℓ's, remove the drift component from $Z(x)$, and infer the covariance from the residuals. Unfortunately, such procedure may lead to a considerably biased covariance - or variogram - estimate. To get

around this difficulty, Matheron developed a theory for non-stationary random functions that he called "Intrinsic Random Functions" (abbreviation IRF). The main practical result is the definition of "generalized covariances" K(h), which, under a restriction, play the same role as ordinary covariances but offer much more flexibility in modeling. In particular, some polynomial models are admissible, and these are especially interesting from the inference point of view, since they involve their parameters in a linear way. In 2-D, valid polynomial generalized covariances are :

$$K(h) = - a_0|h| + a_1|h|^3 \qquad \text{when } m(x) \text{ is a plane}$$

$$K(h) = - a_0|h| + a_1|h|^3 - a_2|h|^5 \qquad " \quad m(x) \text{ is a quadratic}$$

$$(a_0 \geq 0 \ , \ a_2 \geq 0 \ , \ a_1 \geq - (10/3) \sqrt{a_0 \ a_2})$$

The restriction is that K should be used only to calculate the variances of "generalized increments", that is, of linear combinations whose weights are subject to some linear constraints (just as variograms may be used only to calculate variances of simple increments in IRF theory, $- \gamma(h)$ indeed appears as a generalized covariance of order 0).

It is well beyond the scope of this paper to give an account of the IRF theory. The mathematical foundations are given by Matheron, 1973 ; the statistical inference of K is considered by Delfiner, 1975, and Chilès, 1977.

A word now on Kriging. Suppose z(x) is known at sample points $S = \{x_\alpha, x_\beta, \ldots\}$ (S finite) and we want to assess the value $z(x_o)$ at some uninformed point x_o. The kriging estimator $Z^*(x_o)$ is the best linear unbiased estimator (the BLUE) of $Z(x_o)$ based on $Z(x_\alpha)$, $Z(x_\beta), \ldots$ Specifically, denote $Z(x_\alpha)$ by Z_α , $Z^*(x_o)$ by Z_o , and let $Z_o^* = \sum_\alpha \lambda_\alpha Z_\alpha$. The weights λ_α are chosen to satisfy the two conditions :

(1) $\quad E(Z_o^* - Z_o) = 0$ identically in β_ℓ

(2) $\quad E(Z_o^* - Z_o)^2$ minimum

It will be useful for what follows to interpret kriging in a geometrical way. By construction, we are looking for an estimator Z_o^* in the vector space H generated by linear combinations of Z_α, Z_β ,.... :

$$H = \{ \sum_\alpha \lambda_\alpha Z_\alpha \; ; \; x_\alpha \in S \; , \; \lambda_\alpha \text{ real} \}$$

In the general case of a drift $m(x) = \sum_{\ell=0}^{k} \beta_\ell f^\ell(x)$, the unbiasedness condition (1) entails the set of linear constraints

$$(3) \qquad \sum_\alpha \lambda_\alpha f^\ell(x_\alpha) = f^\ell(x_o) \qquad \ell = 0,\ldots,k$$

so that in fact Z_o^* lies in a linear manifold $\mathcal{M}$ contained in H. Now $E(Z_o^* - Z_o)^2$ may be considered as a squared norm $\|Z_o^* - Z_o\|^2$, and it is well known that such a norm is minimized when Z_o^* is the projection of Z_o onto $\mathcal{M}$. (Fig. 1)

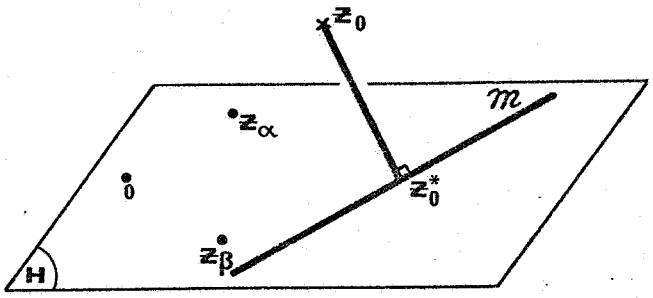

Fig. 1
Projection of $Z(x_o)$ onto the linear manifold $\mathcal{M} \subset H$

It is readily seen that this projection is characterized by the orthogonality relationship

$$(4) \qquad (Z_o - Z_o^*) \perp \sum_\alpha \nu_\alpha Z_\alpha$$

for any set of weights ν_α satisfying

$$(5) \qquad \sum_\alpha \nu_\alpha f^\ell(x_\alpha) = 0 \qquad \ell = 0,\ldots,k$$

When $m(x) \equiv 0$ identically, that is, the constraints (3) are vacuous, then (4) simply says that the error $Z_o - Z_o^*$ is uncorrelated with any sample value Z_α. When $m(x) \equiv m$, that is, $f^o(x) \equiv 1$ and $k = 0$, (4) is equivalent to

$$(6) \qquad (Z_o - Z_o^*) \perp (Z_\alpha - Z_\beta) \quad \text{for any pair } x_\alpha, x_\beta .$$

In this case, the kriging error is uncorrelated with any increment $Z_\alpha - Z_\beta$. Nicely enough, such increments are the basic quantities used to define variograms. Likewise, $\sum_\alpha \nu_\alpha Z_\alpha$ in (4) is a generalized increment such as those used to define generalized covariances. This circumstance comes into play to construct conditional simulations.

Another property of the kriging estimator, which makes it appropriate for contour mapping purposes, is that at data points it coincides with the actual measured values. Indeed, when $x_o \in S$, say $x_o = x_\alpha$, then $Z_o = Z_\alpha$ and $Z_o^* = Z_\alpha$ obviously minimizes $\|Z_o^* - Z_o\|^2$, which is then zero. In general, $\sigma_K^2(x_o) = \|Z_o^* - Z_o\|^2$, the kriging variance, is not zero and can serve as a basis to draw error maps.

3 - THE PRINCIPLES OF CONDITIONAL SIMULATIONS

We start from the following decomposition :

$$(7) \qquad \underbrace{z(x)}_{\text{true value}} = \underbrace{z^*(x)}_{\substack{\text{Kriging} \\ \text{estimate}}} + \underbrace{[z(x) - z^*(x)]}_{\text{error}}$$

(We use lower-case letters for realizations and capital letters for the corresponding random functions). In (7), the error $z(x) - z^*(x)$ remains unknown when $x \notin S$, because the true value $z(x)$ is not available. Suppose now that we are able to simulate realizations of a random function $S(x)$, having the same covariance as $Z(x)$. Then, on a particular simulation $s(x)$ it is possible, with the same pattern of data points, to compute kriging estimates and write similarly :

$$(8) \qquad s(x) = s^*(x) + [s(x) - s^*(x)]$$

This time, the error $s(x) - s^*(x)$ can be known exactly. The idea is to substitute in (7) the error measured on $s(x)$ and define :

$$(9) \qquad z_s(x) = z^*(x) + [s(x) - s^*(x)]$$

We claim that $z_s(x)$ is a conditional simulation, with the properties mentioned in the introduction. Clearly, at data points $z_s(x)$ coincides with the known values since, if $x = x_\alpha$, say, then

$$z^*(x_\alpha) = z(x_\alpha) \qquad \text{and} \qquad s^*(x_\alpha) = s(x_\alpha)$$

There remains to show that $Z_S(x)$ has the same covariance (generalized covariance) as $Z(x)$. This results immediately from the orthogonality property of the kriging estimator. (e.g. Delfiner, 1975). To make things clear, suppose that $m(x) = m$, and let us show that $Z_S(x)$ and $Z(x)$ have the same variogram.

By the independence of $Z(x)$ and $S(x)$:

$$(10) \qquad E[Z_S(x) - Z_S(y)]^2 =$$

$$= E[Z^*(x) - Z^*(y)]^2 + E\{[S(x) - S^*(x)] - [S(y) - S^*(y)]\}^2$$

On the other hand, $Z(x) - Z^*(x)$ and $Z(y) - Z^*(y)$ are orthogonal to $Z^*(x) - Z^*(y)$, which is a linear combination of $Z(x_\alpha)$ satisfying $\sum_\alpha \nu_\alpha = 0$. Therefore :

$$(11) \qquad E[Z(x) - Z(y)]^2 =$$

$$= E[Z^*(x) - Z^*(y)]^2 + E\{[Z(x) - Z^*(x)] - [Z(y) - Z^*(y)]\}^2$$

As by assumption $S(x)$ and $Z(x)$ have the same variogram, the terms between braces in (10) and (11) are equal and

$$E[Z_S(x) - Z_S(y)]^2 = E[Z(x) - Z(y)]^2$$

Intuitively speaking, the whole procedure is based on the idea that since the kriging estimator and the error are uncorrelated, we are entitled to pick an error from a simulation and bluntly add it to the actual estimate.

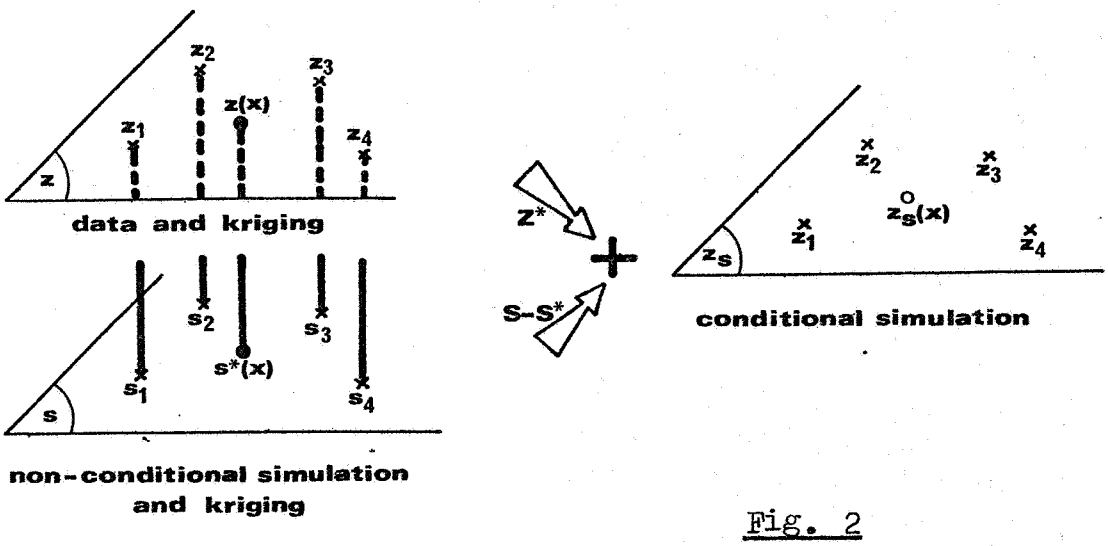

Fig. 2

The only question left is how to obtain non-conditional simulations with a given covariance or variogram. In one dimension, the problem is relatively well solved. But in 2 or 3 dimensions it gets more complicated and the mere extension of 1-D methods would be very costly in terms of computing time. A very elegant and efficient method is the so-called "turning bands" method developed by Matheron and his group at Fontainebleau. Its presentation is relegated to the Appendix.

The relationships between reality, conditional simulation and kriging are well illustrated on the 1-D example of Fig. 3. The solid black line is the real curve ; it passes through data points marked by big dots. The thin line represents the kriging estimates : it goes through the data points but is much smoother than reality. The dashed line is a conditional simulation : it also goes through the data points, but in addition has a variability similar to that of reality. We can notice that in general the kriging estimate is closer to the real value than the simulation. This point should be emphasized : conditional simulations do not purport to estimate reality, but to reproduce its spatial variations, while remaining consistent with the observed data.

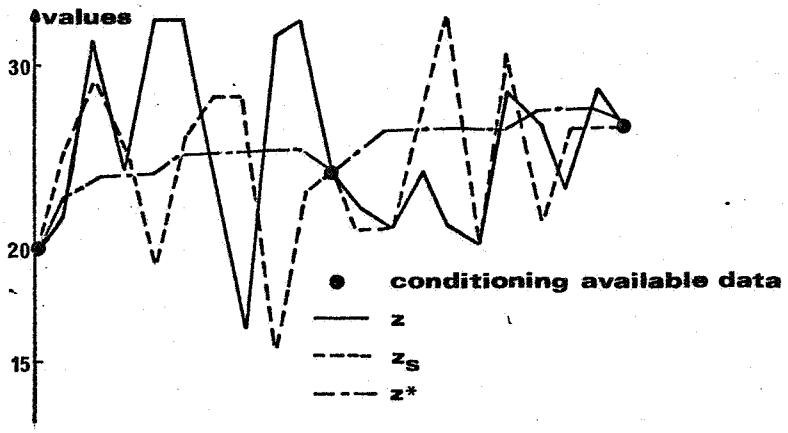

Fig. 3 : Reality - Simulation - Kriging

It is also interesting to note that for a given set of data the average of many conditional simulations at a point x is simply the kriging estimate, and their variance the kriging variance. Indeed, from

$$Z_S(x) = Z^*(x) + [S(x) - S^*(x)]$$

it is clear that

$$E(Z_S(x) | Z_\alpha, Z_\beta \ldots) = Z^*(x)$$

and $$Var(Z_S(x) | Z_\alpha, Z_\beta \ldots) = Var(S(x) - S^*(x)) = \sigma_K^2(x)$$

The variability of a conditional simulation about the kriging estimate reflects precisely the uncertainty attached to that estimate.

4 - A CASE STUDY.

We consider the same oil reservoir as that studied by Haas and Jousselin, 1975, with a more elementary simulation method. It has the shape of a well marked dome, with a maximum thickness of around 140 m. and a lateral extension of the order of 3 or 4 Km. At the base of the reservoir, there is a water table, and the

transition zone is particularly important. Therefore, the oil porosity is considerably smaller in the lower layers.

Altogether 84 wells were drilled, but due to the early time of the discovery, modern geophysical methods had not been used, so that good correlations between wells are lacking. The reservoir was thus simply divided into 7 horizontal layers of 20 m. thickness each (Fig. 4).

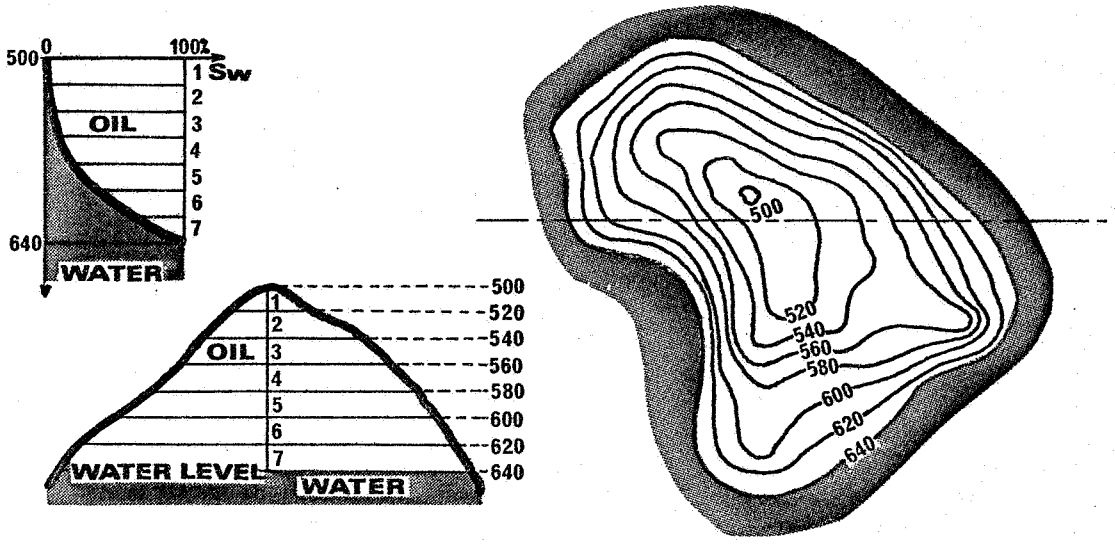

Fig. 4 : Estimation by layers (From Haas and Jousselin, 1975)

The average oil porosity of each layer has been estimated by kriging and the results are reported in Table 1. To simplify matters here, we will assume that these porosities are the true ones, and will concentrate on the error due to the uncertainty about the reservoir boundaries. The simulation part will thus really concern rock volumes, the conversion to oil volumes being done through multiplication by that fixed porosity profile.

Layer	Number of Wells	Average Oil Porosity
1	5	7.8
2	15	6.2
3	23	7.0
4	32	7.2
5	29	5.5
6	16	3.7
7	12	2.1

TABLE 1

Kriging estimates
(From Haas and Jousselin)

The geometric uncertainty originates from two sources : the depth of the top and the depth of the water level. The latter is evaluated to lie between 620 m. and 640 m., that is, in layer 7. As for the top depth, it is found to be modeled best by a quadratic drift and the following generalized covariance :

$$K(h) = - 978 \, |h| + 1070 \, |h|^3 \qquad (|h| \text{ in Km})$$

A regular grid with a spacing of 200 m. × 200 m. is superimposed on the field and kriging estimates are computed at its nodes, as well as standard deviations of the errors (i.e. $\sigma_K(x)$). The contour maps plotted with a printer are shown in Fig. 5 b) and c).

Then, 30 different conditional simulations of the top depth are produced. Their mean and standard deviation are drawn in Fig. 5 d) and e). With 30 simulations only, the mean is almost perfectly equal to its theoretical expectation, the kriged map. The agreement for standard deviations is also good, although in this case sampling fluctuations are higher, a fact easily explained by basic statistical considerations. A few simulations are shown in Fig. 6, as they appear after cut-off below the lowest water level (640 m.). The digits represent the numbers of the layers ; the blanks between layers are just there to enhance visualization. The simulations have been picked out to scan the range of rock volumes, starting from the minimum at the upper right hand corner (n° 16) and increasing counter-clockwise to the maximum (n° 29) ; n° 20 corresponds to the median volume and n° 11 and 13 to the 25% and 75% percentiles. Simulation n° 28 had been added for its particular shape looking somewhat like South America, while the others look like Africa. Altogether, these simulations have a strong family resemblance - which they should if they are to mimic the same reservoir. But in detail the contours are different. In spite of the 84 wells, 19 of which are in the water (below 640 m.), the delineation of the reservoir is still imprecise in the southern and the south-eastern part.

As an illustration of the conditioning effect, Fig. 7 shows cross sections of the kriged top and of the simulations of Fig. 6, along a line AB where estimation variances are low (see the string

Fig. 5

a) Locations of the wells

b) Kriged isobaths to the top (Contour interval 20 m.)

c) Kriging standard deviations (Contour interval 10 m.)

d) Pointwise means of 30 conditional simulations

e) Pointwise standard deviations of these simulations

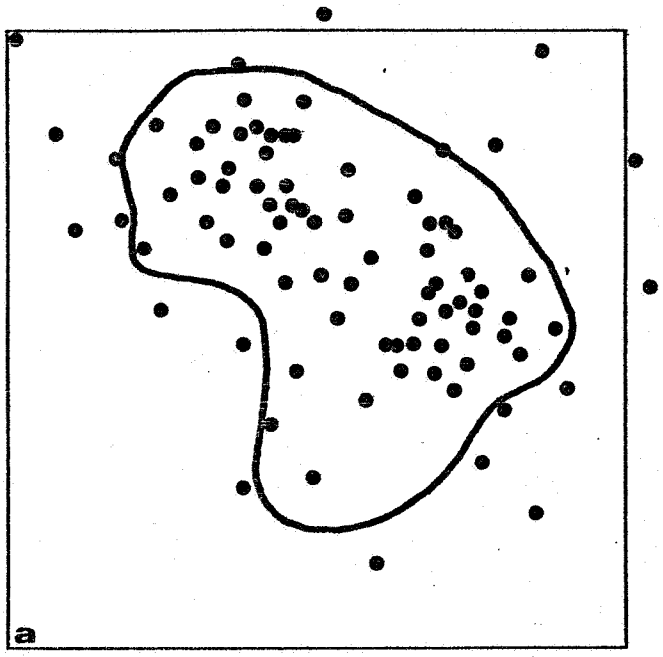

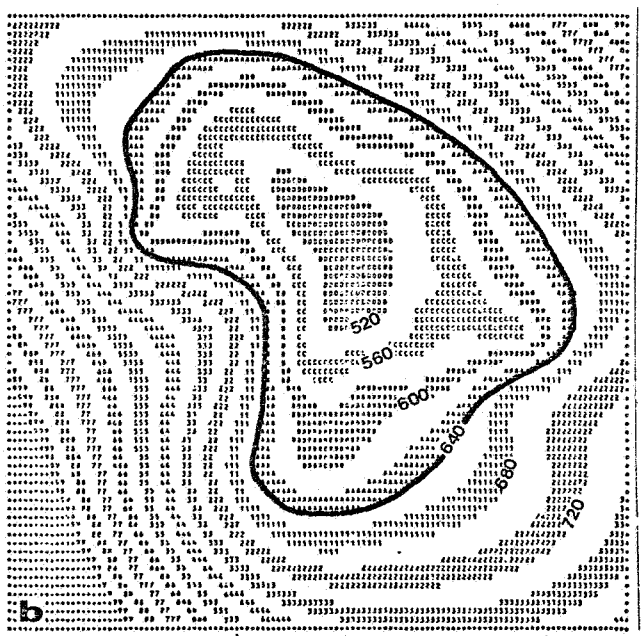

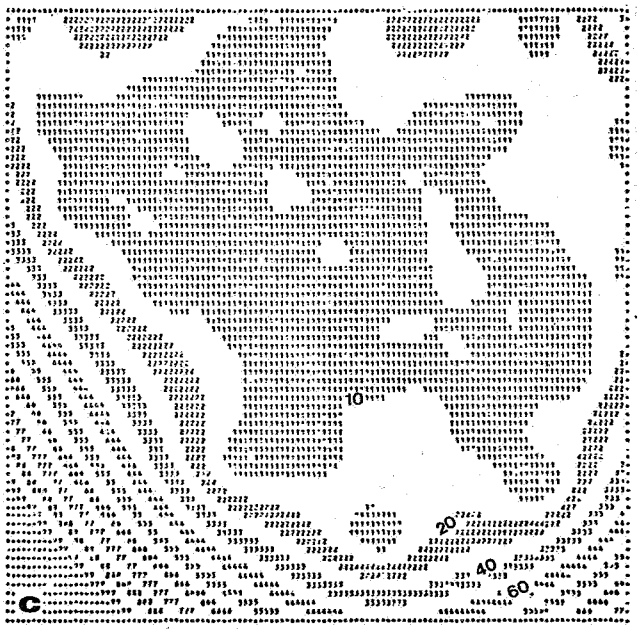

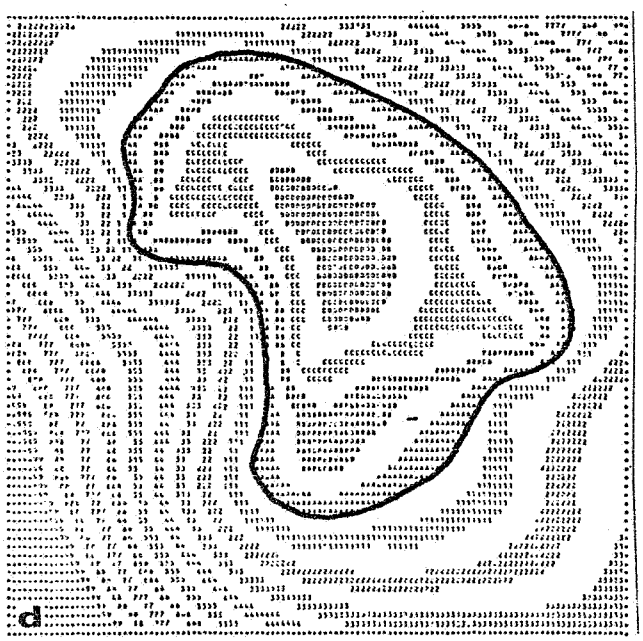

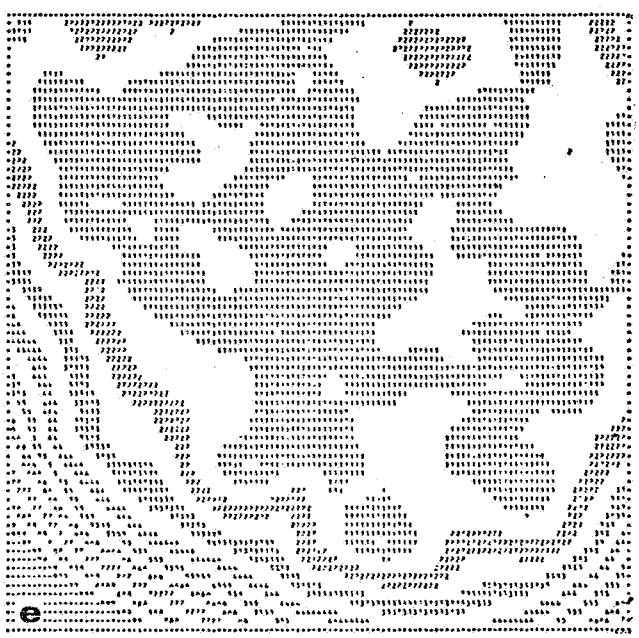

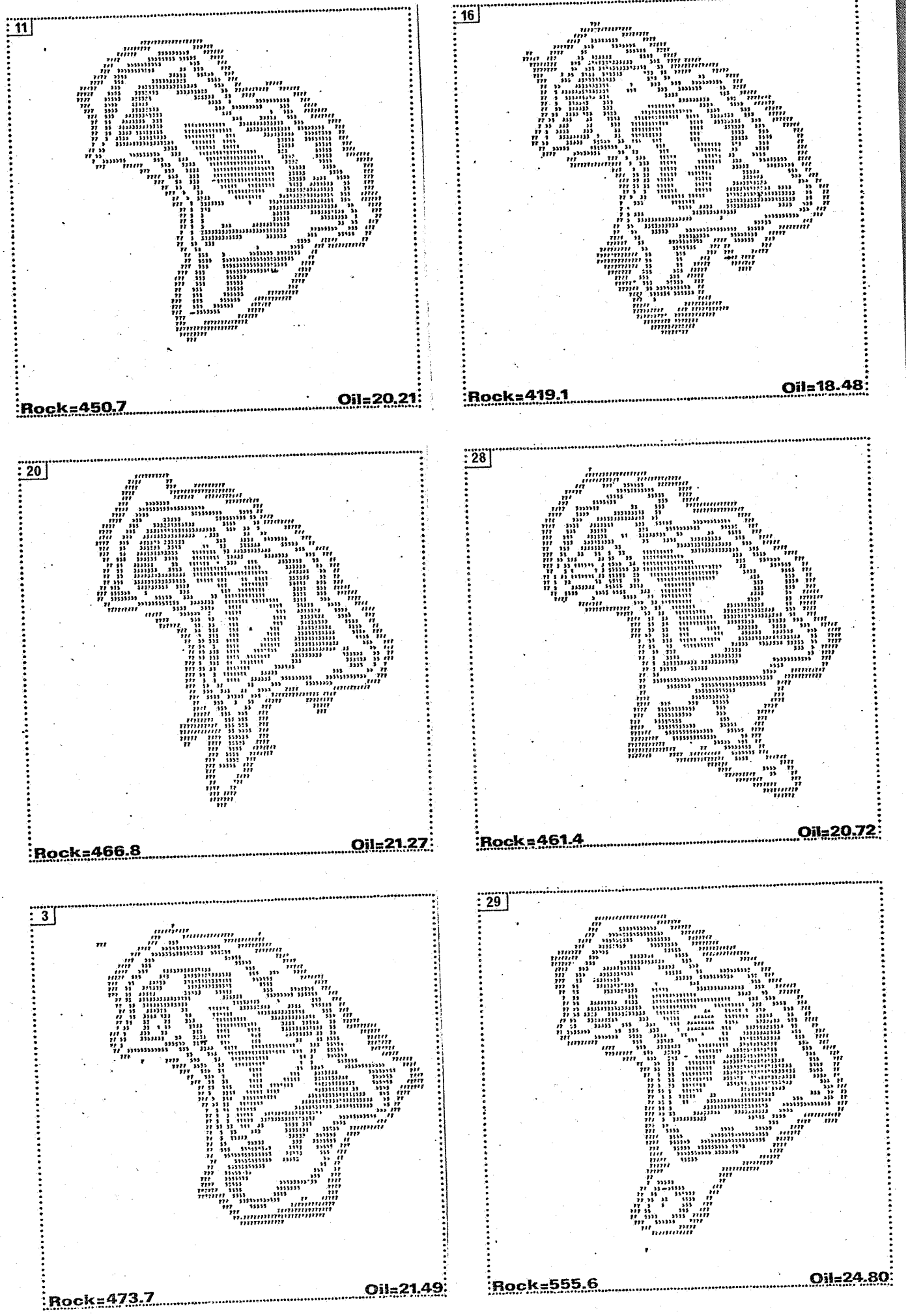

Fig. 6 : Simulated reservoir contours - Cut-off 640 m.
(Rock and oil volumes in 10^6 m^3)

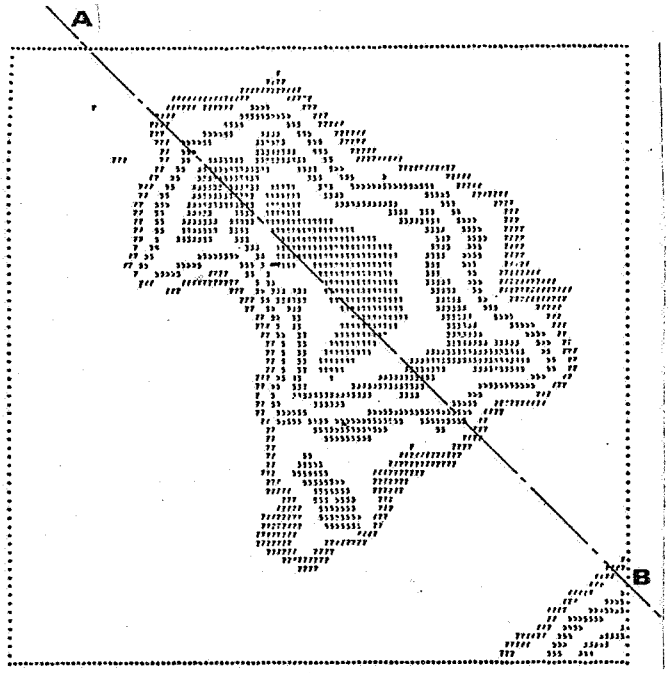

Fig. 7 : Cross-section AB

Below : Kriging estimates and confidence limits

Others : Conditional simulations of Fig. 6 and examples of resurgences.

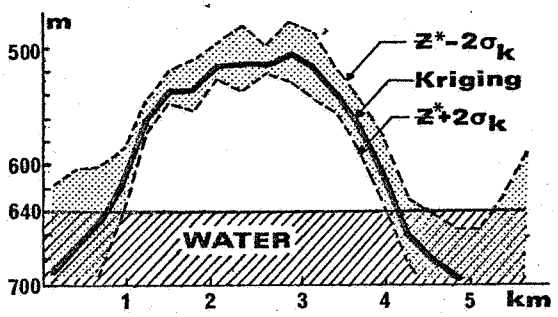

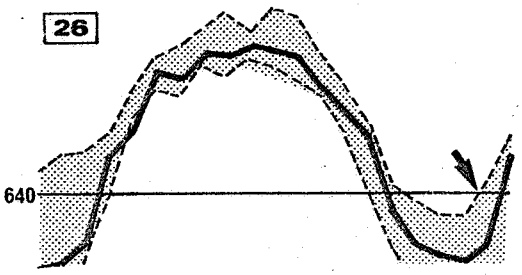

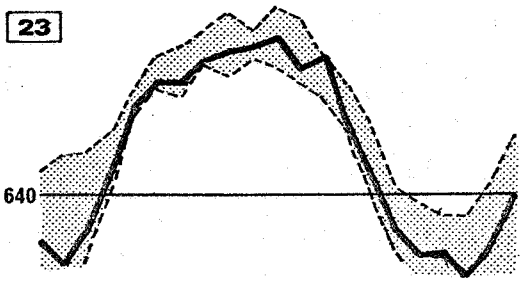

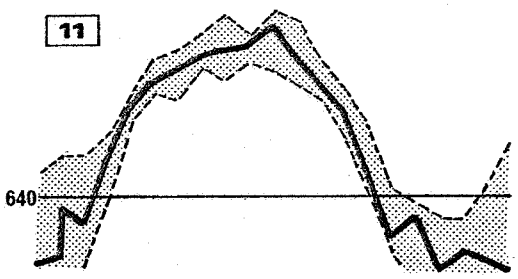

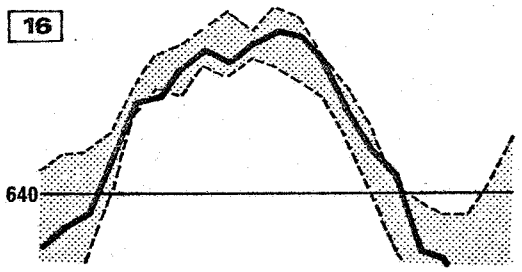

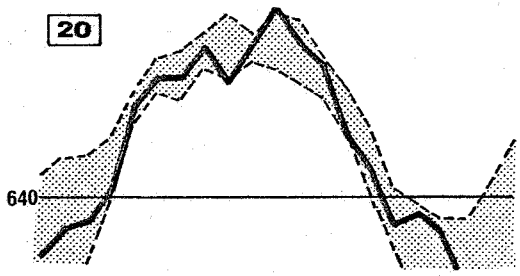

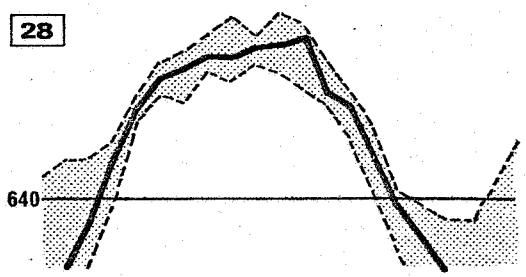

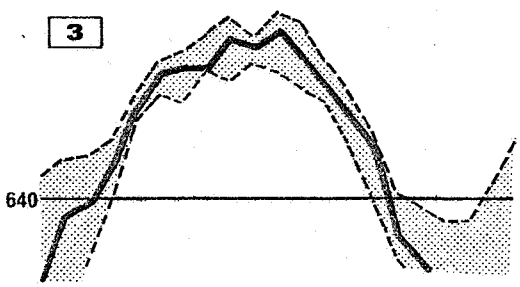

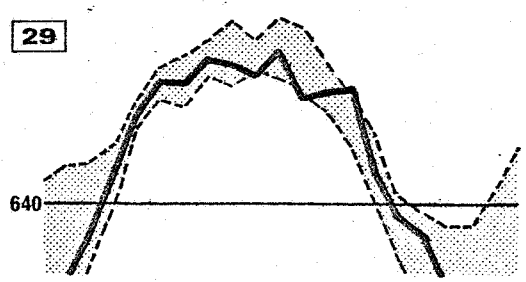

of holes in Fig. 5 c). The simulated profiles fluctuate about the kriged curve, but are more chaotic, and even exhibit sudden downfalls ; these are actually consistent with those observed from some of the well data, and probably due to faults. In general, the simulated profiles remain within the $\pm$ 2 σ_K confidence limits. If a sample point had been located on AB (hence $\sigma_K = 0$), then all profiles would go through it. From the $Z^* - 2\,\sigma_K$ limit of Fig. 7, one may expect that some simulations will show a resurgence of the reservoir above the water level in the southeastern part ; indeed such effect is observed on simulation n° 26 and almost on n° 23. In reality, this is an artefact due to the steep rise in kriging variance as one moves away from the well sites.

Rock and oil volumes have been calculated by numerical integration on the 30 simulations, under three assumptions for the depth of the water level : 620 m., 630 m., 640 m. The results are recorded in Table 2, in the order of the simulation numbers. These volumes have also been evaluated on the basis of the kriged top contour. In the present case, the estimates turn out to be quite comparable to those derived by averaging over simulations. There is no guarantee, however, that it should be so in general, because the cutting off below water level is a non-linear operation. The rock volume, for example, is the integral :

$$V_R = \int_{R^2} [Z_{WL} - Z(x)]\; 1_{\{Z(x)<Z_{WL}\}}\, dx$$

where Z_{WL} is the water level depth and $1_{\{Z(x)<Z_{WL}\}}$ the function assuming the value 1 if $Z(x) < Z_{WL}$ and 0 otherwise. This integral is clearly not linear in $Z(x)$ and the estimator based on kriging :

$$(12) \qquad V_R^* = \int_{R^2} [Z_{WL} - Z^*(x)]\; 1_{\{Z^*(x)<Z_{WL}\}}\, dx$$

does not necessarily satisfy $E(V_R^* - V_R) = 0$. The same holds for the volume of oil.

In addition to this risk of a bias, the estimator V_R^* of (12) leads to rather intractable variance calculations ; in practice,

VOLUMES COMPUTED FROM CONDITIONAL SIMULATIONS

Water Level 620 m		Water Level 630 m		Water Level 640 m	
Rock Volume 10^6 m^3	Oil Volume 10^6 m^3	Rock Volume 10^6 m^3	Oil Volume 10^6 m^3	Rock Volume 10^6 m^3	Oil Volume 10^6 m^3
325.7	17.64	391.1	19.01	463.9	20.54
332.7	18.49	395.9	19.82	467.0	21.32
337.9	18.64	402.3	19.99	473.7	21.49
331.4	18.11	395.9	19.46	467.6	20.97
324.7	17.72	393.1	19.15	468.2	20.73
350.7	19.25	417.0	20.65	489.6	22.17
314.7	17.21	377.0	18.53	446.6	19.99
354.3	19.47	423.0	20.91	498.7	22.50
317.5	17.23	382.7	18.60	454.6	20.11
325.7	17.97	388.6	19.29	459.8	20.79
317.8	17.42	382.3	18.77	450.7	20.21
316.7	17.55	376.6	18.80	445.0	20.24
352.7	19.36	419.3	20.75	490.2	22.25
332.9	18.17	401.1	19.60	475.9	21.17
320.8	17.68	387.8	19.09	466.3	20.73
290.6	15.78	351.3	17.05	419.1	18.48
333.9	18.45	400.7	19.86	473.4	21.39
316.8	17.18	379.8	18.51	447.7	19.93
346.8	19.07	416.0	20.52	492.4	22.13
335.3	18.51	398.4	19.83	466.8	21.27
316.2	17.28	386.3	18.75	465.0	20.41
332.0	18.18	397.3	19.55	467.8	21.03
312.9	17.06	375.3	18.37	443.6	19.81
305.6	16.71	368.2	18.03	436.2	19.46
330.3	18.04	399.6	19.49	476.2	21.10
341.8	18.70	411.7	20.17	488.1	21.77
318.9	17.43	383.0	18.78	453.3	20.26
323.0	17.81	387.8	19.17	461.4	20.72
391.0	21.34	470.1	23.01	555.6	24.80
391.2	21.33	468.9	22.97	554.1	24.75
m	331.4	18.16	397.6	19.55	470.6	21.08
σ	21.1	1.17	24.7	1.24	28.4	1.31

VOLUMES COMPUTED FROM KRIGED RESERVOIR TOP

332.1	18.27	396.2	19.62	465.7	21.08

- T A B L E 2 -

one gives up, and this is a serious drawback.

The histograms of oil in place volumes are shown in Fig. 8. They seem to be skewed to the right - though more simulations should be made to be quite positive about this. For a fixed water level, the distribution of reserves is not very dispersed : the coefficient of variation σ/m is 6%.

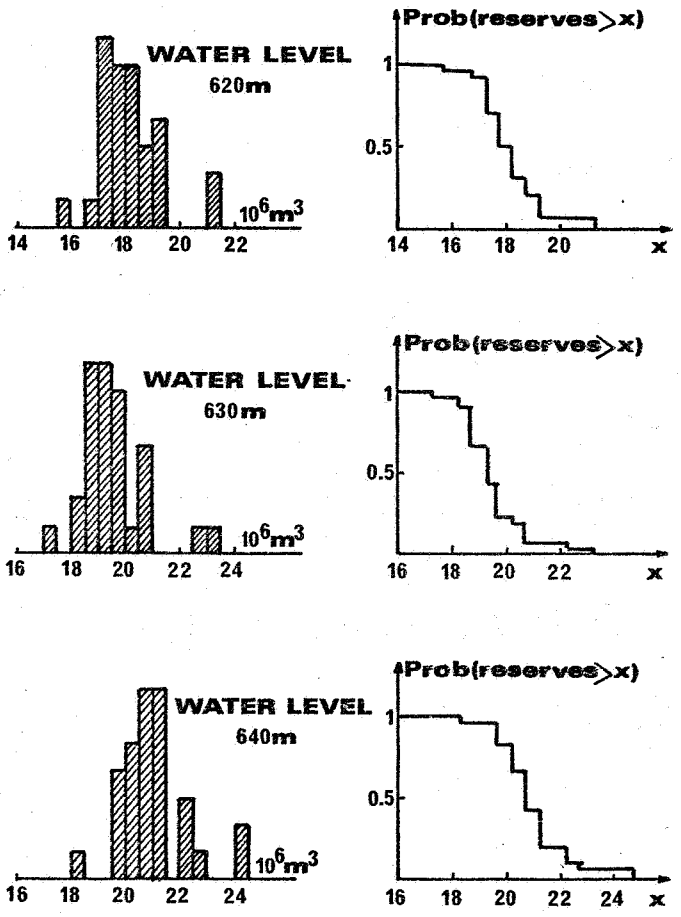

Fig. 8 - Histograms and expectation curves of oil in place volumes.

The conclusion at this point is that the uncertainty on the depth of the reservoir top does not have a large influence on the reserve estimates. This is due to the unusually large number of wells. As for the effect of the uncertainty about the water level, it is dampened by the low porosity of layer 7 : when the water level rises from 640 m. to 620 m., the rock volume decreases by 30%

but the oil volume by 14% only. In order to combine these two sources of uncertainty (top and water level) one may randomize the water level according to a probability distribution, for example a triangular one. But altogether, the geometry is well enough determined and it is certainly necessary to give oil porosities more attention.

5 - REWRITING HISTORY

As pointed out already, the number of wells is unusually large. So, it is interesting to see what our idea of the reservoir would have been on the basis of, say, the first 25 wells. Considering the picture derived from 84 wells as reality, wa can compare. Then, we may try to put on the field developer's shoes and find the best location for the next few wells, with the intention to minimize the uncertainty about the reserves. Of course, we are aware that the game is not fair. For one thing, the developer seeks to optimize production, and not only the evaluation of reserves ; the regular spacing of most of the wells in the center part of the structure proves it (Fig. 9). But also, our choice is guided by what we know from all of the wells. Still, these reservations being made, the results are quite striking.

The covariance that fits best with 25 wells is $K(h) = 6430\ |h|^3$ ($|h|$ in Km.), a quadratic drift being forced into the model. Kriging of the top surface and 30 conditional simulations are done using this covariance. Fig. 9 a shows that the reservoir closes well to the North, but not to the South. The rock and oil volumes are in Table 3 (the heading "simulation" stands for the mean of 30 simulations, and similarly for "σ"). The volumes calculated from kriging are in good agreement with the true ones, but simulations yield estimates that are 1.7 times larger for rock volumes, and 3 times larger for oil volumes. Note though, that these figures are consistent with the huge σ values. Such overestimation of the volumes is due to the lack of sufficient closure of the reservoir ; high variances make some of the simulations "go wild". Incidentall

the display of these unrealistic simulations indicates where drilling wells would most reduce the uncertainty.

If we use the covariance in h and h^3 inferred from the 84 wells, the contours go too far to the Northwest (Fig. 9 b). Volumes estimates derived from kriged isobaths are still good - this time a little overestimated - but the simulation volumes are 1.6 times too large for rock volumes and 3 times for oil volumes. The reason is the same as before.

Fig. 9 c shows the kriged isobaths when two additional wells are taken into account, those drilled n° 46 and n° 75 in chronological order. N° 46, to the North, is in the water (z = 651 m.) and n° 75, to the South, is in the reservoir (z = 588 m.). The closure is much improved, and simulation volumes are of the order of 1.15 times too large for rock and 1.35 for oil.

Suppose now that instead of N° 75 we drill n° 79, in the water (z = 681 m., Fig. 9 d). The closure is this time very good and the simulation volumes are undistinguishable from those obtained using 84 wells. The striking conclusion is that one could have achieved the same accuracy with 27 wells as with 84 ! The price to pay is only the drilling of two wells in the water. Admittedly, it is hard to convince a developer to drill in water on purpose, but on the other hand, such wells bring valuable information on the extension of the reservoir.

Altogether it emerges that with few wells, estimates based on the kriged top are more reliable than those derived from conditional simulations ; we see in Fig. 9 that kriging at least ensures the closure of the reservoir - in this case, not always ! - whereas some of the simulations do not close. But we also see on the 27 (2) example that when this effect is eliminated, these simulations give better estimates than kriging, which systematically underestimates the volume.

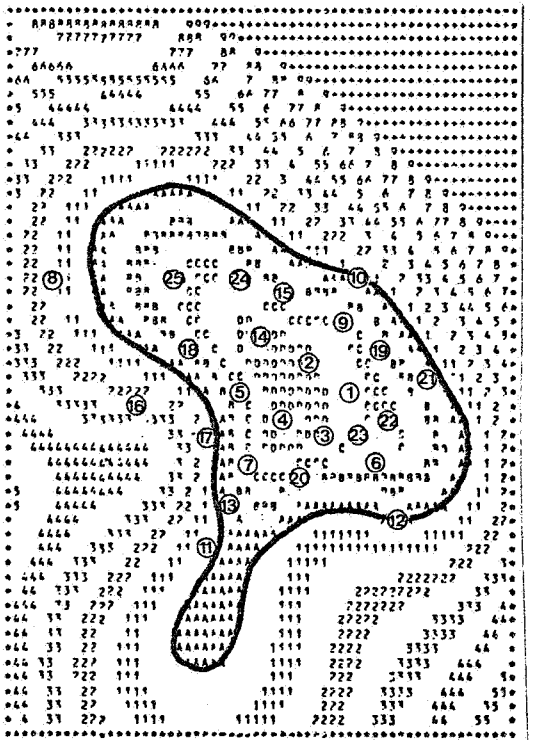

a) - 25 wells - h^3

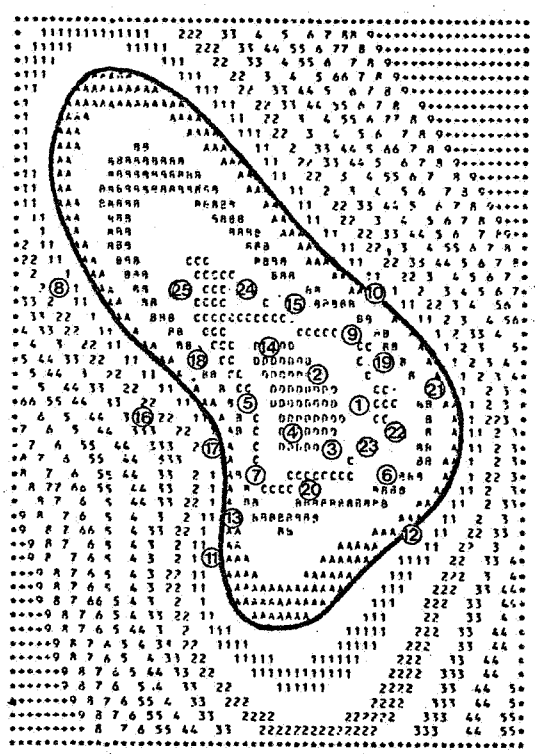

b) 25 wells - h and h^3

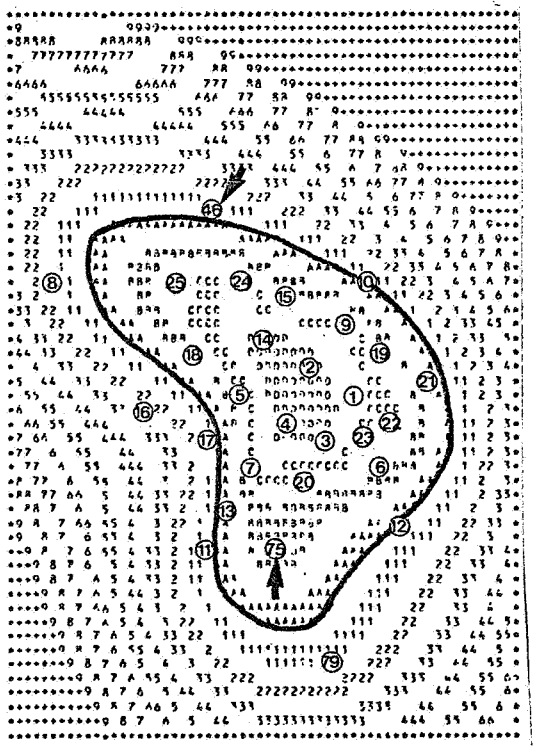

c) 27 wells (1) - h and h^3

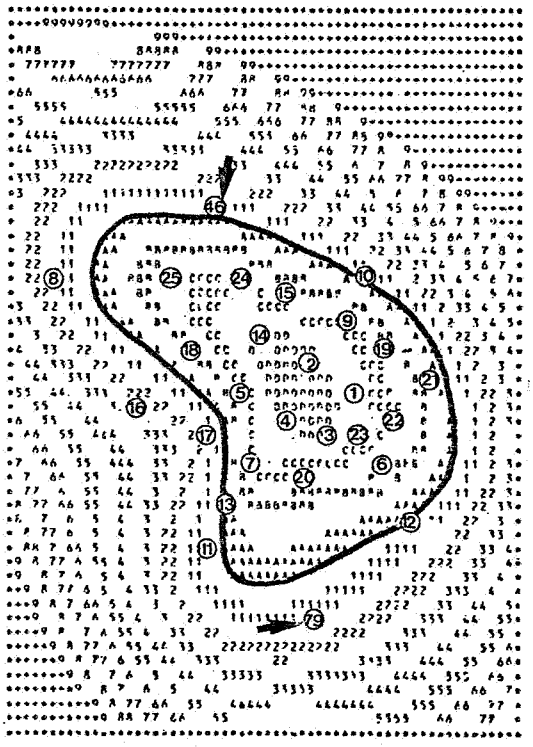

d) 27 wells (2) - h and h^3

Fig. 9 : Kriged isobaths to the top and locations of the first 25 wells ; arrows mark additional wells.

R O C K		WATER LEVEL 620 m.			WATER LEVEL 630 m.			WATER LEVEL 640 m.		
Data	Covariance	Kriging	Simulation	σ	Kriging	Simulation	σ	Kriging	Simulation	σ
84 wells	h and h^3	332.1	331.4	21.1	396.2	397.6	24.7	465.8	470.6	28.4
25 wells	h^3	319.2	576.8	155.4	378.9	705.2	197.3	447.6	841.8	240.6
25 wells	h and h^3	358.0	525.5	156.3	439.9	642.4	192.1	533.0	768.0	228.1
27 wells(1)	h and h^3	314.8	373.9	72.8	380.1	455.5	88.3	452.3	545.5	105.1
27 wells(2)	h and h^3	302.8	324.6	44.7	362.7	394.9	54.5	430.0	473.2	65.3

O I L		WATER LEVEL 620 m.			WATER LEVEL 630 m.			WATER LEVEL 640 m.		
Data	Covariance	Kriging	Simulation	σ	Kriging	Simulation	σ	Kriging	Simulation	σ
84 wells	h and h^3	18.27	18.16	1.17	19.62	19.55	1.24	21.08	21.08	1.31
25 wells	h^3	17.69	62.76	34.42	18.95	65.46	35.26	20.39	68.33	36.13
25 wells	h and h^3	19.23	58.12	41.59	20.95	60.57	42.24	22.91	63.21	42.89
27 wells(1)	h and h^3	17.18	24.51	12.12	18.55	26.23	12.40	20.07	28.12	12.70
27 wells(2)	h and h^3	16.67	18.22	4.11	17.92	19.70	4.29	19.34	21.34	4.49

TABLE 3 - Rock and Oil volumes estimates and the number of wells

6 - CONCLUSIONS

The method of conditional simulations is a new tool to deal with the uncertainty associated with fragmentary reservoir description data . Its main feature is to incorporate the information already available : values observed at the wells and spatial correlations. Conditional simulations may be displayed to suggest hypotheses or interpretations to the geologist ; they can also give indications about appropriate locations for new wells. The simulated values may be integrated to calculate volumes in place and build expectation curves.

To give a computing time order of magnitude, the current simulation program SIMPACK takes 1/250th of a second per grid point and per simulation, on a CDC 6600 computer, or 1/150th on an IBM 370-158 For example, the case study presented here, with $24 \times 24 \times 30 = 17\ 280$ values to simulate, required 70 seconds of CPU time on CDC 6600, or 115 seconds on IBM 370-158.

The method may be further developed in several directions. One is to take several variables into account, including the relations between them (for example thickness, porosity, saturation). A comparison of results and costs should then be made with standard Monte Carlo routines.

Another direction is to remedy the boundary problem for poorly closed reservoirs. It is indeed usually possible to decide for a maximal contour which no simulation should overstep. One method being considered, is to translate this information, and possibly some other of geological origin, into "subjective data" with uncertainty. The kriging and simulation approaches can then handle such lower quality data easily.

Lastly, it seems that it might be interesting to use conditional simulations as input grids to reservoir production models based on history matching techniques (see Chavent and al., Gavalas and al.). The idea is to realize that, although permeabilities are highly variable, they usually show some kind of spatial structure which it would possibly pay off to enter into the production model.

ACKNOWLEDGEMENTS.

The authors are indebted to Elf Aquitaine Company, who supplied the data, and to Mr. M. Mollier for his kind assistance on the case study.

- A P P E N D I X -

GENERATION OF NON-CONDITIONAL SIMULATIONS : THE TURNING BANDS METHOD

The problem is to generate realizations of a random function S(x) on R^n, with a given covariance K(h). There are methods based on Fourier Analysis, on moving averages, or, in discretized form, on the diagonalization of the covariance matrix. However, it is simpler and less costly to use the following "turning bands" method. For pedagogical reasons, we will explain it in the case that K(h) is the ordinary covariance of a weakly stationary random function S(x), with mean zero (abbreviation SRF). The results remain true when K stands for a generalized covariance, and even turn out to be simpler to apply, due to the admissibility of polynomial covariance models.

The idea is to reduce the simulation problem in R^n to a simulation problem in R^1. A naive approach to extend a SRF Y(x) on a line L to the space R^n would be to simply ascribe to each point x of R^n the value of Y at the foot of the perpendicular dropped from x onto L (Fig. 10 a).

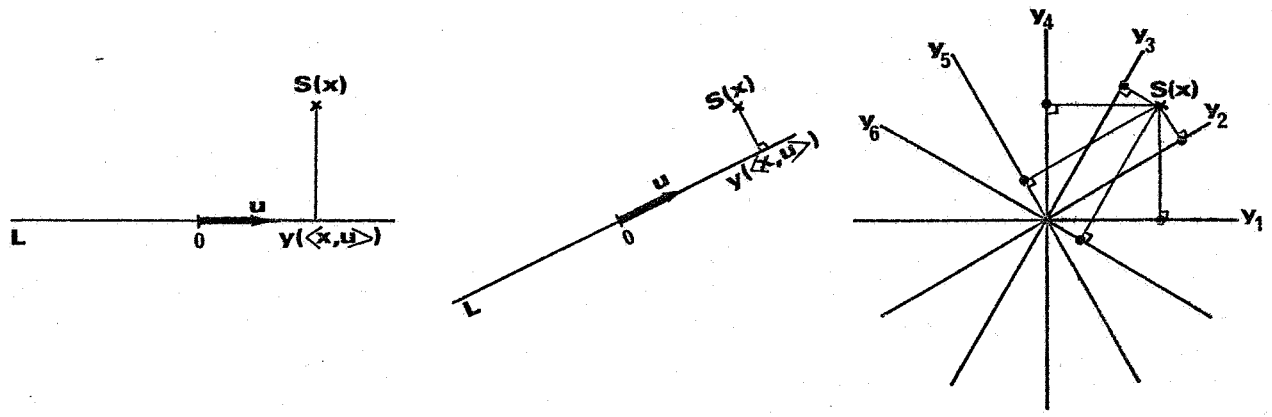

a) u fixed b) u randomized c) independent simulations

Fig. 10 - The theoretical steps of the turning bands method

Let u denote a unit vector in R^n and $< x,u >$ the usual scalar product of x and u in R^n ; K_1 is the covariance of Y and is assumed to be continuous.

$$S_u(x) = Y(< x,u >)$$

is a SRF on R^n and its covariance is

$$E(S_u(x)\ S_u(y)) = K_1\ (< x-y,u >)$$

But we do not like it because it is too anisotropic. Moreover, all realizations of $S_u(x)$ are constant on hyperplanes.

But suppose now that the direction u is chosen at random, uniformly on the unit sphere S_n of R^n, that is, according to the probability distribution ω_n , concentrated on S_n, and invariant by rotations. $S_u(x)$ is then changed into a SRF S(x) whose covariance is

$$K(x-y) = \int K_1\ (< x-y,\ u >)\ \omega_n(du) \qquad (13)$$

As $< x-y,\ u >$ and ω_n are invariant under rotations, K(x-y) does not depend on the orientation of the vector x-y : K is isotropic. Hence, there exists a function K_n on R^+ such that $K(x-y) = K_n(|x-y|)$. Let $x-y = h = r\ u_h$ with $r = |h|$ and u_h a unit vector $\in S_n$. (13) writes

$$K_n(r) = \int K_1(r < u_h,\ u >)\ \omega_n(du) \qquad (14)$$

and, as noticed, does not depend on u_h .

(14) defines an operator $T_n : K_1 \rightarrow K_n = T_n\ K_1$, called the <u>turning bands operator</u>, that associates an isotropic covariance on R^n to each (symmetric) covariance on R^1. The key property of T_n is to be one-to-one (Matheron, 1973). Given a continuous K_n , there exists a unique continuous covariance K_1 on the line such that (14) holds. In R^2 and R^3 formula (14) gives :

$$K_2(r) = \frac{2}{\pi} \int_0^{\pi/2} K_1\ (r \cos \theta)\ d\theta \qquad (15)$$

$$(16) \qquad K_3(r) = \frac{1}{r} \int_0^r K_1(t)\, dt$$

(16) can easily be inverted :

$$K_1(r) = \frac{d}{dr} [r\, K_3(r)]$$

But there is no straightforward solution in R^2. We can note, however, that for all n and any $\alpha > 0$ the function r^α is an eigenfunction of T_n :

$$T_n\, r^\alpha = \text{constant} \times r^\alpha$$

a property that makes simulation of polynomial generalized covariances particularly simple. For $\alpha = 2p+1$, the constant is :

$$B_{n,p} = p!\, \Gamma(\tfrac{1}{2} n) \,/\, (\Pi^{1/2}\, \Gamma(p + \tfrac{1}{2}(1+n)))$$

Coming back to our actual simulation problem, it may seem that this randomization of u is just a theoretical artifice, since realizations of S(x) are still constant on lines or planes. The next step is to approximate the spherical average (14) by a discrete average over N lines, with directions u_i "equally spaced" on the unit sphere. To achieve good convergence properties, independent SRF $Y_i(x)$, with the same covariance K_1, are simulated on each line L_i and one takes

$$S(x) = (S_1(x) + S_2(x) + \ldots + S_N(x)) \,/\, \sqrt{N}$$

where $S_i(x) = Y_i\ (< x, u_i >)$

The covariance of S(x) is

$$(17) \qquad K_n(|h|) = \frac{1}{N} \sum_i K_1\ (< h, u_i >)$$

In 2-D the number of lines may be chosen arbitrarily ; for example the SIMPACK program uses N = 180 . In 3-D the question is more complex ; standard practice is to take the N = 15 lines joining the midpoints of opposite edges of a regular icosahedron - the icosahedron is the regular convex polyhedron with the maximum number of

faces (20) (Guibal, 1972). Naturally, (17) is only a discrete approximation of (14), but the possible bias - depending on h - is small compared with the natural fluctuations of the simulated random functions.

SIMULATION OF AN IRF WITH POLYNOMIAL GENERALIZED COVARIANCE.

The last problem left at this point is the generation of the $Y_i(x)$ on the lines, with the appropriate covariance K_1. Again, several methods may be considered, the most general of which, for SRF's, is based on the spectral representation of Y(x) by mean of an orthogonal random measure (e.g. see Koopmans, p. 41). But in practice, this method requires a fast vanishing spectral measure, that is, a smooth SRF Y(x). Another technique based on moving averages is applicable whenever $K_1 = f * \check{f}$ is the auto-convolution of some function f by its transposed $f(t) = f(-t)$ (see Journel, 1974). We shall merely here sketch the technique used to simulate IRF's on the line, with a given polynomial covariance.

We start from the general representation of a k-IRF on R^1 with polynomial generalized covariance (Matheron, 1973) :

$$(18) \quad Y(x) = b_o\, W(x) + b_1 \int_o^x W(\xi)d\xi + \ldots + b_k \int_o^x \frac{(x-\xi)^{k-1}}{(k-1)!}\, W(\xi)d\xi$$

where W(x) is a 0-IRF with covariance $K(x) = -|h|$ (linear variogram) ; for example W(x) may be chosen as a Wiener-Lévy process (Brownian motion). The wonderful consequence of (18) is that <u>it suffices to simulate a single process W(x)</u> and adapt the coefficients $b_o, b_1, \ldots, b_k$. For example, when k = 2, (quadratic drift)

$$K_1(h) = -a_o|h| + a_1|h|^3 - a_2|h|^5 \qquad (a_o \geq 0,\ a_2 \geq 0,\ a_1 \geq -2\sqrt{a_o a_2})$$

and b_o, b_1, b_2 must be chosen to satisfy

$$a_o = b_o^2 \ , \quad a_1 = b_1^2 - 2\, b_o\, b_2 \ , \quad a_2 = b_2^2$$

For k = 1, (linear drift) let $b_2 = 0$.

W(x) itself may be simulated on a segment [-R, +R] in different ways. The simplest, used in SIMPACK, is the following (Chilès, 1977 b) : take x_o at random on [-R, +R], with a uniform distribution, and a random value c from a distribution with mean zero and variance σ^2. Let

$$W(x) = c \; 1_{\{x_o(x-x_o) > 0\}}$$

It is easy to check that for x and x+h in [-R, +R] :

$$E(W(x+h) - W(x))^2 = \sigma^2 |h| \; / \; 2R$$

Looking at a realization of W on a single line this procedure seems crude, but averaging over a large number of lines endows S(x) with a reasonable behavior.

Note that all realizations are zero at the center of the figure, as well as their derivatives up to order k.

REFERENCES

CHAVENT, G., DUPUY, M., LEMONNIER P., 1975 - "History Matching by use of Optimal Control Theory". Society of Petroleum Engineers Journal, Feb. 1975, pp.74-86.

CHILES, J.P., 1975 - "How to adapt Kriging to non-classical problems". Advanced Geostatistics in the Mining Industry.- D. Reidel Publ. Co., Dordrecht, Holland, pp.69-89.

CHILES, J.P., 1977a- "SIMPACK, Notice d'Utilisation" (Proprietary package).

CHILES, J.P., 1977b- " Géostatistique des phénomènes non stationnaires dans le plan".- Thèse, Université de Nancy.

DELFINER, P., DELHOMME, J.P., 1973 - "Optimum Interpolation by Kriging". Display and Analysis of Spatial Data, Wiley and Sons, London, pp. 96-114.

DELFINER, P., 1975 - "Linear estimation of non-stationary spatial phenomena".- Advanced Geostatistics in the Mining Industry.- D. Reidel Publ. Co., Dordrecht, Holland, pp. 49-68.

GAVALAS, G.R., SHAH, P.C., SEINFELD, J.H., 1976.- "Reservoir History Matching by Bayesian Estimation". - SPE - AIME paper n° 5740.

GUIBAL, D., 1972 - Simulation de schémas intrinsèques".- Centre de Géostatistique, Fontainebleau.- Tech. Report No. 291.

HAAS, A., JOUSSELIN, C., 1975 - "Geostatistics in Petroleum Industry". Advanced Geostatistics in the Mining Industry.- D. Reidel Publ. Co., Dordrecht, Holland, pp. 333-347.

HAAS, A., MOLLIER, M., 1974 - "Un aspect du calcul d'erreur sur les réserves en place d'un gisement".- Revue de l'Institut Français du Pétrole, Vol. XXIX, n° 4, pp. 507-527.

HAAS, A., VIALLIX, J.R., 1976 - "Krigeage applied to Geophysics - The answer to the problem of estimates and contouring".- Geophysical Prospecting, Vol. XXIV, n° I, pp. 49-69.

JOURNEL, A.G., 1974 - "Geostatistics for Conditional Simulation of Orebodies".- Economic Geology, Vol. 69, pp. 673-687.

KOOPMANS, L.H., 1974 - "The Spectral Analysis of Time Series".- Academic Press, New York and London.

MATHERON, G., 1973 - "The Intrinsic Random Functions and their Applications", Advances in Applied Probability 5, pp. 438-468.

Additional References on Geostatistics.

MATHERON, G., 1965 - "Les Variables Régionalisées et leur Estimation". Masson et Cie, Paris.

MATHERON, G., 1971 - "The Theory of Regionalized Variables and its Applications".- Cahiers du C.M.M., n° 5, Fontainebleau, France.

DAVID, M., 1977 - "Geostatistical Ore Reserve Estimation".- Elsevier, Amsterdam, the Netherlands.

DELHOMME, J.P., 1976 - "Applications de la Théorie des Variables Régionalisées dans les sciences de l'Eau".- Thèse, Université Paris VI.

JOURNEL, A.G., HUIJBREGTS, Ch., 1978 - "Mining Geostatistics".- To be published by Academic Press, New York and London.